Eur. Phys. J. A **26**, 153–157 (2005)
DOI 10.1140/epja/i2005-10174-3

THE EUROPEAN PHYSICAL JOURNAL A

Letter

Lifetime measurement in ^{74}Kr and ^{76}Kr

A. Görgen[1,a], E. Clément[1], A. Chatillon[1], A. Dewald[2], W. Korten[1], Y. Le Coz[1,b], N. Mărginean[3], B. Melon[2], R. Menegazzo[4], O. Möller[2], Ch. Theisen[1], D. Tonev[3,c], C.A. Ur[4], and K.O. Zell[2]

[1] DAPNIA/SPhN, CEA Saclay, F-91191 Gif-sur-Yvette Cedex, France
[2] Institut für Kernphysik, Universität zu Köln, D-50937 Köln, Germany
[3] INFN-Laboratori Nazionali di Legnaro, I-35020 Legnaro (Padova), Italy
[4] Dipartimento di Fisica, Università di Padova and INFN Sezione di Padova, I-35131 Padova, Italy

Received: 24 October 2005 / Revised version: 16 November 2005 /
Published online: 1 December 2005 –
Communicated by D. Schwalm

Abstract. Lifetimes of excited states in the ground-state bands of ^{74}Kr and ^{76}Kr were measured using the recoil-distance Doppler-shift and the differential decay curve methods. The states were populated in the ^{40}Ca(^{40}Ca, $\alpha 2p$) and ^{40}Ca(^{40}Ca, $4p$) reactions. Gamma rays were detected with the GASP array which was coupled to the Cologne Plunger device. The results resolve discrepancies between earlier lifetime measurements and a recent Coulomb excitation experiment. Experimental transition rates are compared to theoretical calculations. The results support a strong mixing between prolate and oblate configurations for the low-spin states, and represent an important basis for the interpretation and understanding of the shape coexistence phenomenon in this mass region.

PACS. 21.10.Re Collective levels – 21.10.Tg Lifetimes – 27.50.+e $59 \leq A \leq 89$

The proton-rich krypton nuclei near the $N = Z$ line exhibit some of the best examples for shape coexistence in nuclei. The competition of prolate and oblate shapes in this mass region is caused by large shell gaps that occur both for oblate and prolate quadrupole deformations at proton and neutron numbers 34, 36, and 38. Several theoretical models predict coexisting prolate and oblate states in the nuclei with these proton and neutron numbers [1–7]. While the different approaches generally agree on the equilibrium shapes involved, they find different results for the precise excitation energies of the states and the transition rates between them.

An experimental indication for shape coexistence (in even-even nuclei) is the observation of low-lying excited 0^+ states. Such a state can be understood as a "second ground state" corresponding to a coexisting shape different from that of the ground state. Such states are indeed observed throughout the chain of light even-even Kr isotopes between ^{72}Kr and ^{80}Kr. Their excitation energy decreases with decreasing neutron number to a minimum in ^{74}Kr, and increases again in the self-conjugate nucleus ^{72}Kr. The 0_2^+ states in ^{72}Kr and ^{74}Kr are isomeric (*i.e. shape isomers*) and decay via $E0$ transitions to the ground state [8–10]. The rotational cascades of the ground-state bands are strongly distorted at low spin, pointing to a mixing of the prolate and oblate configurations. The mixing amplitudes can be inferred from an extrapolation of the rotational bands at high spin. This analysis shows for the ground state of ^{74}Kr a maximum mixing of the oblate and prolate configurations which are almost degenerate [10]. Together with the energy dependence of the excited 0^+ states and the electric monopole strengths $\rho^2(E0)$ of the transitions to the 0^+ ground states, this suggests an inversion of the ground-state shape from prolate in the heavier isotopes to oblate in ^{72}Kr.

This scenario has recently been confirmed by a direct measurement of the spectroscopic quadrupole moments of states in ^{74}Kr and ^{76}Kr through low-energy Coulomb excitation with radioactive beams [11,12]. A large number of both transitional and diagonal matrix elements for the two isotopes was determined in this measurement. The results for the transitional matrix elements are partly in conflict with previously measured lifetimes, in particular for the 4^+ state in ^{74}Kr [13]. On the other hand, the precise

[a] e-mail: agoergen@cea.fr
[b] *Present address*: DEN/DTN/SMTM, CEA Cadarache, F-13108 Saint-Paul-lez-Durance Cedex, France.
[c] *Present address*: Institute for Nuclear Research and Nuclear Energy, BAS, 1784 Sofia, Bulgaria.

knowledge of the transitional matrix elements is needed in this case of Coulomb excitation with weak radioactive beams in order to be sensitive to the reorientation effect, and therefore to determine the spectroscopic quadrupole moments (including the sign of the deformation).

In order to resolve the discrepancies between the recent Coulomb excitation results and the previously published lifetimes, a new measurement of lifetimes has been performed in ^{74}Kr and ^{76}Kr using the recoil-distance Doppler-shift method (RDDS). A higher precision was expected from the new measurement, as the lifetime data in the literature for low-spin states in both ^{74}Kr [13] and ^{76}Kr [14–16] are based on singles measurements which suffered from contaminations from other reaction products and unknown side feeding. Several lifetime measurements employing the Doppler-shift attenuation method (DSAM) have been performed for ^{74}Kr [17–19] and ^{76}Kr [20–22]. They are, however, not sensitive to the relatively long lifetimes below the 6^+ state in the respective ground-state bands.

The present RDDS measurement was performed using the Cologne Plunger device [23] coupled to the γ spectrometer GASP [24] at the Laboratori Nazionali di Legnaro. Excited states in ^{74}Kr and ^{76}Kr were populated in the reactions ^{40}Ca(^{40}Ca, $\alpha 2p$)^{74}Kr and ^{40}Ca(^{40}Ca, $4p$)^{76}Kr at a nominal beam energy of 147 MeV. The target consisted of a 800 μm/cm^2 thick layer of ^{40}Ca evaporated onto a Au foil of 2 mg/cm^2 that was facing the beam. The downstream side of the target was also covered by a thin Au layer of approximately 100 μg/cm^2 in order to prevent oxidation. Slowed down in the support layer and the target itself, the average beam energy at the center of the target was 124 MeV. The recoils had an average velocity $v/c = 3.50(5)\%$ and were finally stopped in a Au foil of 12 mg/cm^2 thickness. Data were collected for 13 different distances between the target and the stopper foil ranging from 7.5 μm to 1500 μm, with an average of 12 hours beam on target for each distance. Gamma rays were detected with the GASP array, which, for this experiment, comprised 32 Compton-suppressed Ge detectors in the so-called configuration II, *i.e.* in a close geometry without the BGO scintillators of the inner ball. Most of the detectors were placed at forward and backward angles where the sensitivity to the Doppler shift is highest. For the data analysis the detectors were grouped into seven rings with respect to the beam axis. Events were recorded when at least two Compton-suppressed Ge detectors gave coincident signals. For the off-line analysis the data were sorted into $\gamma\gamma$ coincidence matrices. Separate matrices were sorted for all combinations of rings and for all distances.

The spectra in fig. 1 show the first three transitions of the ground-state band in ^{74}Kr for several distances as indicated. The spectra were observed by the first ring of detectors placed at 36° with respect to the beam axis, so that the components of the transitions emitted in flight are shifted to higher energies. All spectra are gated from above on the shifted components of the transitions directly feeding the state of interest. Different gates were used depending on the angle of the detector in which the gating

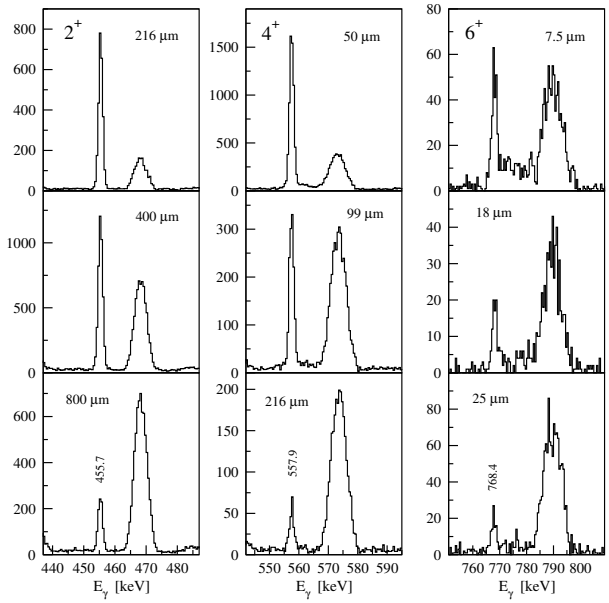

Fig. 1. Gamma-ray coincidence spectra showing the transitions depopulating the 2^+, 4^+, and 6^+ states in ^{74}Kr, observed at 36° with respect to the beam axis for various distances between the target and the stopper foil. See text for details.

transition was observed, and the spectra were then added to result in seven individual spectra, one for each angle under which the depopulating transition was detected. Care was taken to set symmetric gates on the shifted components of the peaks in order to avoid a bias toward faster or slower recoil velocities. This procedure was repeated for all 13 distances. The spectra of the 768 keV transition depopulating the 6^+ state show triple coincidences with a gate on the shifted component of the transition above and an additional gate on either component of the transition below. The triple-coincidence condition eliminated contaminations from cascades with similar transition energies in a negative-parity band of ^{74}Kr and in ^{77}Rb, strongly populated in the $3p$ reaction channel. The intensities of the shifted and stopped components were extracted from these and the corresponding spectra for the other detector angles.

The lifetimes of the states were determined from the intensities of the shifted and stopped components of the transitions using the differential decay curve method [25]. Since the spectra were gated from above, all uncertainties from unknown side feeding are eliminated. The peak intensities of the shifted (sh) and stopped (st) components have to be corrected for differences in the running time and beam intensity for the different distances. The common normalization factors $N(x)$ for each distance were determined from the total number of coincidences for several strong cascades in different nuclei. For coincidences between transitions directly populating and depopulating the state of interest, the lifetime is extracted from the coincidence intensities for each distance as

$$\tau(x) = \frac{\frac{1}{N(x)} I(\gamma_1^{sh}, \gamma_2^{st}, x)}{v \frac{\mathrm{d}}{\mathrm{d}x} \frac{I(\gamma_1^{sh}, \gamma_2^{sh}, x)}{N(x)}}, \qquad (1)$$

Table 1. Summary of the lifetimes in ^{74}Kr and ^{76}Kr measured in the present and in previous RSSD and DSAM experiments.

	I^π	E_γ (keV)	τ (ps)	Previous results (ps)				Adopted	$B(E2)$ (e^2fm^4)
^{74}Kr	2^+	455.7	33.8(6)	28.8(57) [13]	23.5(20) [17]			33.8(6)	1223(22)
	4^+	557.9	5.2(2)	13.2(7) [13]				5.2(2)	2895(111)
	6^+	768.4	1.09(23)	0.91(10) [18]	1.08(14) [19]	0.90(15) [17]		0.96(7)	3169(231)
	8^+	966.9		0.24(4) [18]	0.35(5) [19]	0.28(5) [17]		0.28(3)	3445(324)
	10^+	1144.8		0.16(3) [19]	0.10(3) [17]			0.13(2)	3190(521)
^{76}Kr	2^+	423.7	41.5(8)	36.0(10) [16]	53.4(72) [14]	35.0(30) [15]		41.5(8)	1433(28)
	4^+	610.7	3.67(9)	4.9(4) [16]	5.0(20) [20]	8.2(23) [14]		3.67(9)	2612(64)
	6^+	825.0	0.97(29)	1.5(2) [16]	1.25(12) [20]	1.18(13) [21]	0.86(6) [22]	1.00(5)	2132(107)
	8^+	1019.7		0.33(3) [21]	0.30(3) [20]	0.29(3) [22]		0.31(2)	2411(136)
	10^+	1189.2		0.14(2) [20]	0.144(16) [22]			0.142(12)	2407(211)

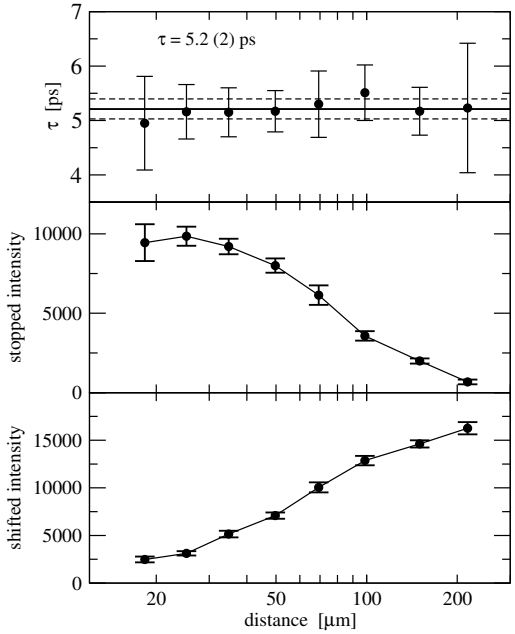

Fig. 2. Example for decay curves of the shifted (bottom) and unshifted (center) components of the transition depopulating the 4^+ state in ^{74}Kr. The intensities are normalized to the distance with the highest level of statistics. The top panel shows the derived lifetimes for each measured distance.

where v is the recoil velocity. Piecewise continuous and differentiable polynomials were fitted to the intensity curves of the shifted components $I(\gamma_1^{sh}, \gamma_2^{sh}, x)$ in order to determine their derivatives. An example for the stopped and shifted intensity curves is shown in fig. 2 for the 4^+ state in ^{74}Kr together with the resulting lifetime of the state. The differential decay curve method gives an independent value for the lifetime for each target-to-stopper distance that lies within the sensitive range for this particular lifetime according to eq. (1). A scattering or slope of the lifetime values for different distances would indicate the presence of systematic errors. As this is not the case, the values can be combined in a weighted mean value. The six rings of the GASP spectrometer at forward and backward angles also give independent measurements of the lifetimes. The results for the different rings are very consistent and were combined to give the final lifetime. The results are summarized and compared to previous measurements in table 1.

The lifetimes of the 2^+ and 4^+ states in both ^{74}Kr and ^{76}Kr were measured for the first time with a large array of Compton-suppressed germanium detectors in the present work. Considering the difficulties arising from contaminations from other reaction products and unknown side feeding in the earlier singles measurements, it is not surprising that considerable differences were observed. In a singles measurement the analysis is also complicated by γ-rays following the radioactive decay of the recoils that accumulate in the stopper foil. The $2^+ \rightarrow 0^+$ transition in the decay product ^{76}Se, for example, has an energy of 559.1 keV, compared to 557.9 keV for the $4^+ \rightarrow 2^+$ transition in ^{74}Kr. The stopped component of this transition therefore appears too strong in a singles spectrum, resulting in a too long lifetime. This can easily be verified with the present data when they are analyzed in singles. It may be suspected that the very long lifetime for the 4^+ state in ^{74}Kr of 13.2(7) ps reported in ref. [13] is due to this effect, whereas in the present coincidence measurement such contaminations can be excluded, and a much shorter lifetime of 5.2(2) ps is found. Since the lifetimes measured in a singles measurement depend on those of the states above, it is then not surprising that the lifetime of the 2^+ state in ^{74}Kr reported to be 28.8(57) ps in ref. [13] is shorter than that of 33.8(6) ps found in this work. The only other measurement for the 2^+ state [17] used only one target-to-stopper distance, which is not enough to determine the lifetime and can at most give a rough estimate. The new lifetime results for the 2^+ and 4^+ states in ^{76}Kr do not agree with any of the previously measured values, even though the differences are not quite as severe as in the case of ^{74}Kr. Again, the new lifetime for the 4^+ state is shorter and that of the 2^+ state longer than the previously published values.

For the 6^+ states in both ^{74}Kr and ^{76}Kr the lifetimes are already so short that they become comparable to the slowing-down time in the stopper foil. As can be seen in fig. 1, the stopped component is therefore not a symmetric Gaussian peak anymore, but has a tail from the γ-rays that were emitted during the slowing-down process of the recoils. However, at least for the spectra from the most forward and backward detectors at 36° and 144°,

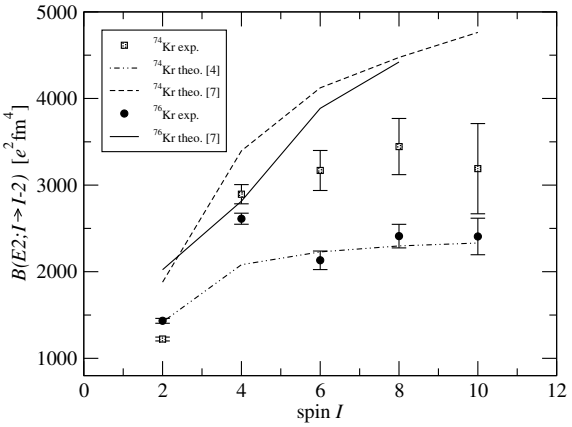

Fig. 3. Experimental and theoretical reduced transition probabilities $B(E2; I \to I-2)$ for ^{74}Kr and ^{76}Kr.

the two components are well enough separated and the spectra clean enough (in triples) to distinguish the different components and include the tail in the intensity of the stopped peak, as required by the differential decay curve method. The distances between the target and the stopper foil were, however, chosen to give the best sensitivity for longer lifetimes around 5 ps. With only few distances sensitive to short lifetimes around 1 ps and the additional uncertainty from the slowing-down effect, the lifetimes for the 6^+ states are less accurate than those of the longer-lived states. The agreement with the results from Doppler-shift attenuation measurements both in ^{74}Kr [17–19] and ^{76}Kr [20–22] is satisfying, in particular in consideration of the fact that DSAM measurements generally suffer from systematic uncertainties from the treatment of the stopping powers, which can be as large as 20%, and which do not affect the precision of the RDDS measurement. The agreement between the values extracted with both techniques gives additional confidence in the results. Because of the significantly improved experimental conditions that permitted to determine the lifetimes of the 2^+ and 4^+ states in both isotopes with high precision, the new values are adopted in the following discussion, ignoring the previously published results. For the 6^+ states, on the other hand, the weighted mean of all RDDS and DSAM measurements is used.

The $B(E2)$ values for the lowest transitions in the ground-state bands in ^{74}Kr and ^{76}Kr are plotted in fig. 3. They are compared to the values found for the lowest prolate bands in recent theoretical works using the complex Excited Vampir approach [4] and to configuration mixing calculations of particle-number– and angular-momentum–projected mean-field states from Skyrme-Hartree-Fock-Bogolyubov calculations [7]. The two principal observations are the much reduced transition strengths for the $2^+ \to 0^+$ transitions and the generally higher values for ^{74}Kr. The first can be attributed to the strong mixing of prolate and oblate configurations in the 0^+ and 2^+ states, which has also been observed experimentally in particular for ^{74}Kr [10]. While the Skyrme beyond-mean-field calculations reproduce this increasing trend qualitatively for ^{74}Kr, they overestimate the experimental values by about 35%. The discrepancy between the calculation and experiment is somewhat larger in the case of ^{76}Kr, and the difference between ^{74}Kr and ^{76}Kr is not reproduced. The Vampir calculations, which are only available for ^{74}Kr, on the other hand, underestimate the $B(E2)$ values. They, too, reproduce the increase very well. It seems that both calculations describe the mixing of the prolate and oblate wave functions correctly, while the absolute size of the deformation seems to be too large in the Skyrme calculations and too small in the Vampir ones.

The new lifetime results, in particular that for the 4^+ state in ^{74}Kr, are not in conflict anymore with the transitional matrix elements found in the Coulomb excitation experiments with radioactive ^{74}Kr and ^{76}Kr beams [11, 12]. The rather precise knowledge of the lifetimes can be used as constraint in the analysis of the Coulomb excitation data and thus enhances the sensitivity to determine the diagonal matrix elements, *i.e.* the spectroscopic quadrupole moments, for several yrast and non-yrast states in both isotopes [12].

In summary, lifetimes of low-lying states in ^{74}Kr and ^{76}Kr have been measured with high precision in a recoil-distance Doppler-shift experiment. The results resolve discrepancies between previous lifetime measurements and a recent Coulomb excitation experiment. The reduced transition probabilities are compared with theoretical calculations which take into account a mixing between coexisting prolate and oblate states. The results support a strong shape mixing for the 0^+ and 2^+ states, while the absolute value of the deformation is not exactly reproduced by the calculations. The precise knowledge of the lifetimes will give sufficient sensitivity to extract the spectroscopic quadrupole moments from the Coulomb excitation data.

This work was supported in part by the German BMBF under Contract No. 06K167 and by a Marie Curie Fellowship of the European Community program IHP under Contract No. HPMF-CT-2002-02018 (D.T.). Fruitful discussions with P.-H. Heenen are gratefully acknowledged.

References

1. W. Nazarewicz *et al.*, Nucl. Phys. A **435**, 397 (1985).
2. P. Bonche *et al.*, Nucl. Phys. A **443**, 39 (1985)
3. R. Bengtsson, in *Nuclear Structure of the Zirconium Region*, edited by J. Eberth, R.M. Meyer, K. Sistemich (Springer, 1988) p. 17.
4. A. Petrovici *et al.*, Nucl. Phys. A **665**, 333 (2000).
5. P. Sarriguren *et al.*, Nucl. Phys. A **658**, 13 (1999).
6. M. Yamagami *et al.*, Nucl. Phys. A **693**, 579 (2001).
7. M. Bender, P.H. Heenen, private communication and *Shape coexistence in neutron-deficient Kr isotopes*, to be published.
8. C. Chandler *et al.*, Phys. Rev. C **56**, R2924 (1997).
9. F. Becker *et al.*, Eur. Phys. J. A **4**, 103 (1999).
10. E. Bouchez *et al.*, Phys. Rev. Lett. **90**, 082502 (2003).
11. A. Görgen *et al.*, Acta Phys. Pol. B **36**, 1281 (2005).
12. E. Clément *et al.*, to be published in Phys. Rev. C.

13. J. Roth *et al.*, J. Phys. G **10**, L25 (1984).
14. E. Nolte *et al.*, Z. Phys. **268**, 267 (1974).
15. J. Keinonen *et al.*, Nucl. Phys. A **376**, 246 (1982).
16. B. Wörmann *et al.*, Nucl. Phys. A **431**, 170 (1984).
17. S.L. Tabor *et al.*, Phys. Rev. C **41**, 2658 (1990).
18. J. Heese *et al.*, Phys. Rev. C **43**, R921 (1991).
19. A. Algora *et al.*, Phys. Rev. C **61**, 031303(R) (2000).
20. R.B. Piercey *et al.*, Phys. Rev. C **25**, 1941 (1982).
21. C.J. Gross *et al.*, Nucl. Phys. A **501**, 367 (1989).
22. J.J. Valiente-Dobón *et al.*, Phys. Rev. C **71**, 034311 (2005).
23. A. Dewald, in *Ancillary Detectors and Devices for Euroball*, edited by H. Grawe, GSI Report (Darmstadt, 1998) p. 70.
24. D. Bazzacco, in *Proceedings of the International Conference on Nuclear Structure at High Angular Momentum, Ottawa, 1992*, AECL Report 10613, Vol. **2** (1992) p. 376.
25. A. Dewald *et al.*, Z. Phys. A **334**, 163 (1989).